Adsorption (2006) 12:5–18
DOI 10.1007/s10450-006-0134-3

Fixed-bed adsorption of carbon dioxide/methane mixtures on silicalite pellets

José A. Delgado · María A. Uguina · José L. Sotelo · Beatriz Ruíz · José M. Gómez

Received: 22 February 2006 / Revised: 11 April 2006 / Accepted: 7 July 2006

Abstract The adsorption of carbon dioxide and methane on silicalite pellets packed on a fixed bed has been studied. Equilibrium and kinetic measurements of the adsorption of carbon dioxide and methane have been performed, and a binary adsorption isotherm for carbon dioxide/methane mixtures has been obtained. A model based on the LDF approximation for the mass transfer has been used to describe the breakthrough curves obtained experimentally. A PSA cycle has been proposed for obtaining methane with purity higher than 98% from carbon dioxide/methane mixtures containing 38% and 50% methane, and its performance has been simulated using the proposed model. The simulation results show that silicalite can be a suitable adsorbent for employment in a PSA separation process for carbon dioxide removal from coalseam and landfill gases.

Keywords Carbon dioxide, methane, silicalite, adsorption, fixed-bed, PSA simulation

1 Introduction

Carbon dioxide separation from methane is important in the processing of natural gas obtained from coalseam and landfill gases because it reduces the energy content. Moreover, it is not simply an inert, but also can be corrosive. Carbon dioxide must be removed prior to low temperature processing for NGL recovery. Generally, pipeline specifications for natural gas require a carbon dioxide concentration below 2–3%. The coalseam gas primarily contains methane and higher hydrocarbons (30–70%) and additional contaminants such as carbon dioxide and nitrogen (Gomes and Hassan, 2001). Landfill gases contain mainly methane (50–65%) and carbon dioxide (35–50%) as well as small amounts of nitrogen, with many different hydrocarbons and sulfur compounds in trace concentrations (Ruthven et al., 1994). Finally, effluent gas from natural gas wells undergoing carbon dioxide flooding may contain from 20 to 80% of carbon dioxide (Cavenati et al., 2005).

The technology most widely used for carbon dioxide removal is amine absorption, but amine plants are complex and costly. Membrane systems also have been used for this purpose and, within certain process conditions, can be an attractive alternative. Recently, the separation of carbon dioxide/methane mixtures using a SAPO-34 membrane has been studied by Li et al. (2005). However, one challenge for membrane systems is reaching the allowable carbon dioxide levels required by the pipeline system. For this reason, membrane systems are sometimes integrated with further processing. Another alternative is the removal of carbon dioxide by means of an adsorption process. Pressure swing adsorption technology has gained interest due to low energy requirements and low capital investment costs. The main

J. A. Delgado (✉) · M. A. Uguina · J. L. Sotelo · B. Ruíz · José M. Gómez
Department of Chemical Engineering, Universidad Complutense de Madrid, 28040, Madrid, Spain
e-mail: jadeldob@quim.ucm.es

requirement for a PSA cycle to be applicable to the separation of carbon dioxide/methane mixtures is to find an adsorbent selective to one of these compounds. It is also necessary that the affinity of the adsorbent to the selected component is not too high, because otherwise the regeneration step can negatively affect the economy of the process. Also, the uptake rates must be high enough to achieve a reasonable productivity. Separation by PSA can be based either on the different adsorption affinity of the components (equilibrium separation), or on the different diffusion rates in the adsorbent (kinetic separation) (Ruthven et al., 1994, Yang, 1997). A process for the recovery of methane from landfill gases was developed using a narrow-pore carbon molecular sieve (Schroter and Juntgen, 1989, Pilarczyk and Knoblauch, 1988). Carbon dioxide diffuses into the adsorbent much faster than methane, which is obtained as the raffinate product in the effluent stream. A high recovery was reported (over 90%), with a product purity of 87–89%. Kapoor and Yang (1989) have also studied the kinetic separation of a carbon dioxide/methane mixture (50/50) using a carbon molecular sieve, obtaining 90% methane with a recovery of 90% and a productivity of 0.05 kg methane kg adsorbent^{-1} h^{-1}. A maximum purity of 95.5% with 40% recovery was obtained in this work. Gomes and Hassan (2001) have investigated the feasibility of coalseam methane recovery with a VSA process using a carbon molecular sieve as the sorbent, obtaining a 90% methane product from a 50/50 carbon dioxide/methane mixture. Other process using an adsorbent kinetically selective to carbon dioxide for carbon dioxide removal from natural gas (ETS-4 zeolite) is currently offered by Engelhard Corporation. This process is able to treat economically a natural gas containing 38% of carbon dioxide and reduce this concentration below 2% (Engelhard brochure, 2005). Recently, the upgrade of methane from a carbon dioxide/methane mixture by pressure swing adsorption using a Takeda Carbon Molecular Sieve 3K has been studied experimentally by Cavenati et al. (2005). Purity higher than 96% can be obtained with recovery higher than 75% from a 45/55 carbon dioxide/methane mixture, but to obtain purity higher than 98% feed pressure must be increased and recovery is around 65%.

Although some PSA systems which are based on kinetic separation are used at industrial scale at present, such as the one employed in the nitrogen production from air using carbon molecular sieve adsorbents, commonly these systems are based on equilibrium separation, which have the advantage that they do not require a high internal resistance of the sorbent to separate mixtures in which all the components adsorb significantly on the adsorbent. Among all the commercial adsorbents available to perform this separation based on equilibrium separation, zeolites are possible candidates, as they have high selectivities for carbon dioxide, because of the polar character of this adsorbate. The separation of hydrogen/carbon dioxide and carbon dioxide/methane mixtures using 5A zeolite was patented by Sircar and Zondlo (1987). However, carbon dioxide adsorption on these adsorbents is typically too strong, which makes desorption difficult. A further consideration on the selection of the adsorbent concerns possible effects of the impurities in the feed gas, such as water and sulfur compounds. It is desirable that these impurities do not affect carbon dioxide adsorption. Hydrophobic zeolites, such as silicalite and USY, having low aluminum content, show a good compromise between high carbon dioxide selectivity and easy regeneration, according to literature data (Golden and Sircar, 1994, Dunne et al., 1996). As only non-specific interactions (dispersion plus polarization) are involved, the desorption rate of carbon dioxide from these zeolites is significantly higher than from the hydrophilic ones, where the quadrupole moment of carbon dioxide dominates the interaction. Moreover hydrophobic zeolites, unlike their hydrophilic counterparts, can be used in adsorption systems for carbon dioxide removal in the presence of water vapor, as their adsorption capacity is not drastically reduced in this case (Suzuki et al., 1997).

The design of a PSA system requires the development of a model that can describe the dynamics of adsorption on a fixed-bed, taking into account all the relevant transport phenomena. In this work, the adsorption of carbon dioxide and methane on silicalite pellets packed in a fixed bed has been studied. Equilibrium and kinetic measurements of the adsorption of carbon dioxide and methane on this adsorbent have been performed, in order to obtain the monocomponent adsorption equilibrium isotherms. A model based on the LDF approximation for the mass transfer has been used to describe the breakthrough curves obtained experimentally. A PSA cycle has been proposed for obtaining methane with a purity higher than 98% from carbon dioxide/methane mixtures containing 38% and 50% methane, and its performance

has been examined using the model proposed in this work.

2 Experimental section

All the gases used in this work had purity higher than 99.5%, supplied by Praxair. The adsorbent used was a commercial agglomerated silicalite (30% binder) in the form of cylindrical pellets, supplied by CECA. Adsorbent properties are shown in Table 1.

Adsorption experiments were performed by passing gas mixtures through a column packed with the adsorbent. The remaining void column volume was filled with glass beads. Fixed-bed properties are also given in Table 1. A scheme of the experimental setup is shown in Fig. 1.

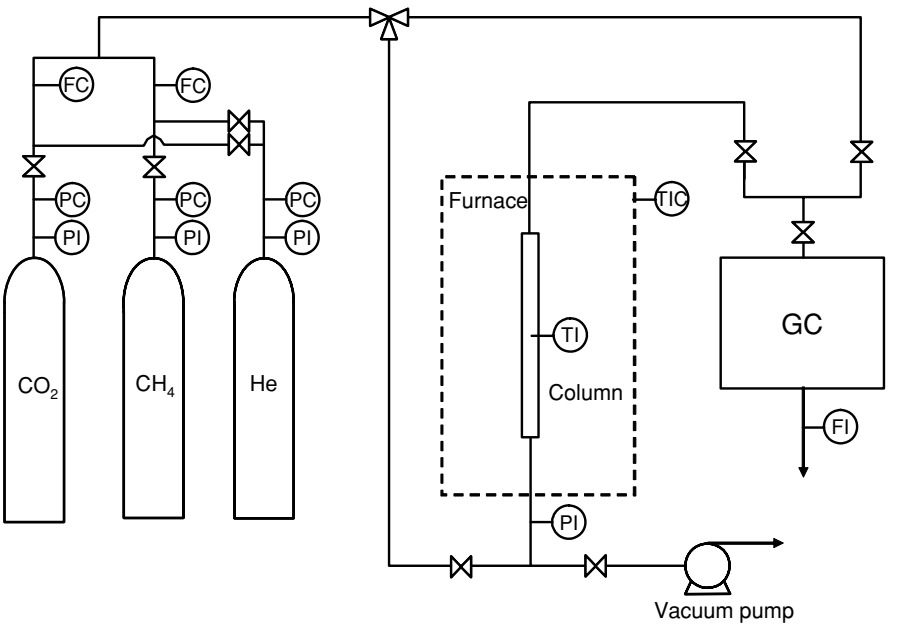

Fig. 1 Scheme of the setup for the fixed-bed adsorption experiments

Table 1 Properties of the adsorbent and the fixed-bed

Adsorbent	
Pellet radius	$R_p = 0.7$ mm (cylindrical)
Pellet length	$L_p \sim 5$ mm
Particle density	$\rho_p = 1070\,\mathrm{kg\,m^{-3}}$
Crystal size	$r_c = 3 \cdot 10^{-6}$ m
[a]Particle macroporosity	$\varepsilon_{macro} = 0.48$ (extracrystalline)
[b]Particle microporosity	$\varepsilon_{micro} = 0.11$ (intracrystalline)
Particle total porosity	$\varepsilon_p = 0.59$
Solid heat capacity	$c_{p,s} = 1000\,\mathrm{J\,kg^{-1}\,K^{-1}}$
Fixed-bed	
Bed length	$L = 0.163$ m
Bed weight	$W = 16.9$ g
Bed internal diameter	$d_i = 0.016$ m
Bed voidage fraction	$\varepsilon = 0.52$
Column wall thickness	$l = 2$ mm
Wall heat capacity	$c_{p,w} = 500\,\mathrm{J\,kg^{-1}\,K^{-1}}$
Wall density	$\rho_w = 8000\,\mathrm{kg\,m^{-3}}$

[a]Estimated by Hg porosimetry (pore volume for pores with diameter larger than 2 nm = 0.45 $\mathrm{cm^3\,g^{-1}}$).
[b]Estimated by nitrogen porosimetry (micropore volume = 0.1 $\mathrm{cm^3\,g^{-1}}$).

The flow of each gas was controlled with mass flow controllers (Bronkhorst). The adsorbent was regenerated after each adsorption experiment by evacuation for 30 min. and feeding helium afterwards for 30 min. The column was located inside a thermostated chamber. The gas flow rate at the bed exit was measured with a bubble meter. Adsorbent temperature was monitored with a thermocouple located at 9 cm from the bed entrance. A Varian 3800 gas chromatograph fitted with a 3 m $\times 1/8''$ stainless steel column packed with Porapak Q (Supelco) and equipped with TCD detector was employed for monitoring the methane and carbon dioxide concentration at the bed exit, using helium as the reference gas. The chromatograph was equipped with a sampling valve with a loop of 0.25 ml, which was continuously filled with the gas entering the chromatograph, and connected to the chromatograph column at different times. All the connections are made of Teflon and stainless steel tubing ($1/8''$).

3 Model description

The model used to describe the fixed-bed dynamics is derived from the mass, energy and momentum balances, including the following assumptions:

(i) The flow pattern is described with the axially dispersed plug flow model
(ii) Local thermal equilibrium is assumed between the gas and the adsorbent particles
(iii) The mass transfer rate is represented by a linear driving force (LDF) model
(iv) The gas phase behaves as an ideal gas mixture
(v) Radial concentration and temperature gradients are negligible

On this basis, the overall mass balance in a differential portion of the fixed bed is given by,

$$\frac{\partial C}{\partial t} = \frac{-1}{\varepsilon L}\left(\frac{\partial u}{\partial x}C + u\frac{\partial C}{\partial x}\right) - \frac{\sum_{i=1}^{i=n} N_i}{\varepsilon} \tag{1}$$

where C is the total gas concentration, t is time, ε is the bed voidage fraction, L is the bed length, u is the superficial velocity, x is the dimensionless axial coordinate, and N_i is the adsorption rate of the ith component. The total concentration is given by,

$$C = \frac{P}{RT_g} \tag{2}$$

where P is the pressure and T_g the gas temperature. The variation of total pressure with time is given by,

$$\frac{\partial P}{\partial t} = RT_g\frac{\partial C}{\partial t} + \frac{P}{T_g}\frac{\partial T_g}{\partial t} \tag{3}$$

The superficial velocity is related to the total pressure gradient according to the Ergun's equation,

$$-\frac{\partial P}{\partial x} = \frac{150L\mu\ (1-\varepsilon)^2}{\varepsilon^3 d_p^2}u + \frac{1.75\,L\ (1-\varepsilon)\,\rho_g}{\varepsilon^3 d_p}u^2 \tag{4}$$

where μ is the gas viscosity, ρ_g is the gas density, and d_p the particle diameter. The rate of adsorption for each component is given by

$$N_i = (1-\varepsilon)\,\rho_p\frac{\partial\overline{q_i}}{\partial t} = (1-\varepsilon)\,\rho_p k_{s,i}\left(q_i^* - \overline{q_i}\right) \tag{5}$$

where $k_{s,i}$ is a lumped mass transfer coefficient, q_i^* is the adsorbed concentration in equilibrium with the gas phase, and $\overline{q_i}$ is the average adsorbed concentration for the ith component. The mass balance for each component gives the variation of the corresponding mole fraction with time,

$$\frac{\partial y_i}{\partial t} = \frac{D_L}{L^2C}\frac{\partial C}{\partial x}\frac{\partial y_i}{\partial x} + \frac{D_L}{L^2}\frac{\partial^2 y_i}{\partial x^2} - \frac{u}{\varepsilon L}\frac{\partial y_i}{\partial x} - \frac{N_i}{\varepsilon C} + \frac{\left(\sum_{i=1}^{i=n} N_i\right)y_i}{\varepsilon C} \tag{6}$$

where D_L is the axial dispersion coefficient. The energy balance in the gas phase gives the variation of gas

temperature with time,

$$\frac{\partial T_g}{\partial t} = \frac{\frac{\lambda}{L^2}\frac{\partial^2 T_g}{\partial x^2} - \frac{u\,C\,c_{p,g}}{L}\frac{\partial T_g}{\partial x} + \sum_{i=1}^{i=n}(1-\varepsilon)\;\rho_p\,(-\Delta H_i)\,\frac{\partial \overline{q_i}}{\partial t} - \frac{2h_w}{R_i}\left(T_g - T_w\right) + \varepsilon\,RT_g\,\frac{\partial C}{\partial t}}{\left(\varepsilon + (1-\varepsilon)\;\varepsilon_p\right)\;C\,c_{v,g} + (1-\varepsilon)\;\rho_p\,c_{p,s}} \tag{7}$$

where λ is the thermal axial dispersion coefficient, R_i is the bed radius, h_w is the heat transfer coefficient between the gas and the wall, T_w is the wall temperature, $(-\Delta H_i)$ is the adsorption enthalpy for the ith component, and c_p and c_v are the heat capacities at constant pressure and constant volume, respectively, for the corresponding phase (g = gas, s = solid). For the column wall, the energy balance leads to,

$$\frac{\partial T_w}{\partial t} = \frac{2\,R_i\,h_w(T_g - T_w) - 2\,R_{ml}\,U\;(T_w - T_{ext})}{\rho_w c_{p,w}[(R_i + l)^2 - R_i^2]} \tag{8}$$

where R_{ml} is the log mean wall radius, U is an overall heat transfer coefficient between the column wall and the external air (Da Silva and Rodrigues, 2001), and T_{ext} is the external air temperature. The boundary conditions for the equations giving the time dependence of P, y_i and T_g (Eqs. (3), (6) and (7)) are the following,

$$x = 0 \quad uC|_{z+} = uC|_{z-} \tag{9}$$

$$x = 1 \quad P|_{z-} = P|_{z+}$$

$$x = 0 \quad -\varepsilon\frac{D_L}{L}C\frac{\partial y_i}{\partial x}|_{z+} + uC\,y_i|_{z+} = uC\,y_i|_{z-} \tag{10}$$

$$x = 1 \quad \left.\frac{\partial y_i}{\partial x}\right|_{z-} = 0$$

$$x = 0 \quad -\frac{\lambda}{L}\left.\frac{\partial T_g}{\partial x}\right|_{z+} + uCc_{p,g}T_g|_{z+} = uCc_{p,g}T_g|_{z-} \tag{11}$$

$$x = 1 \quad \left.\frac{\partial T_g}{\partial x}\right|_{z-} = 0$$

The initial conditions are the following,

$$t = 0 \quad \forall x\,P = P_0 y_i = y_{i0} T_g = T_{ext} T_w = T_{ext} \tag{12}$$

$$\overline{q_i} = \frac{P\;y_{i0}\;\varepsilon_p}{RT\rho_p} + f(P\;y_{i0}, \cdots, P\;y_{n0}, T)$$

where the function f is the multicomponent adsorption equilibrium isotherm. In this expression, the amount of adsorptive retained in the adsorbent pores was included in the adsorbed concentration (Sircar and Kumar, 1983).

The complete model was solved numerically using the PDECOL program (Madsen and Sincovec, 1979), which uses orthogonal collocation on finite elements technique. These model equations (except the adsorption equilibrium isotherm) have been proposed following the work of Da Silva and Rodrigues (2001), introducing several simplifications to reduce the computational time: a lumped mass transfer coefficient has been used instead of considering two mass transfer resistances in a bidisperse adsorbent, and local thermal equilibrium has been considered instead of taking into account the resistance to heat transfer between the adsorbent and the gas in the bed. Further information about the calculation and fitting procedures used in this work can be found elsewhere (Delgado et al., 2002).

4 Results and discussion

4.1 Adsorption equilibrium of carbon dioxide and methane

In order to describe the fixed-bed dynamics of the adsorption of carbon dioxide/methane mixtures on silicalite, the basic information required is the adsorption equilibrium behavior of the pure components. The adsorption equilibrium isotherms of carbon dioxide and methane have been obtained in the fixed-bed setup used for the kinetic experiments, estimating the adsorbed concentration as a function of the feed concentration from a mass balance in the fixed-bed. Different feed concentrations were obtained by mixing in different proportions the adsorbing gas and helium. For each experimental breakthrough curve, the adsorbed concentration is given by,

$$q = \frac{1}{W}\left(QC_F\,t_\infty - \int_0^{t_\infty} QC|_{x=1}dt\right) - \frac{[\varepsilon + (1-\varepsilon)\varepsilon_p]}{\rho_p(1-\varepsilon)}C_F \tag{13}$$

Table 2 Experimental conditions for the runs performed with carbon dioxide-helium and methane-helium mixtures

Run	Adsorbate	P_0 (Pa)	y_F	Q ($m^3\ s^{-1}$)	T (K)	q ($mol\ kg^{-1}$)
1	CO_2	$9.41 \cdot 10^4$	0.08	$3.86 \cdot 10^{-7}$	298	0.152
2	CO_2	$9.62 \cdot 10^4$	0.14	$3.37 \cdot 10^{-7}$	298	0.280
3	CO_2	$9.39 \cdot 10^4$	0.14	$6.99 \cdot 10^{-7}$	298	0.300
4	CO_2	$9.54 \cdot 10^4$	0.21	$3.48 \cdot 10^{-7}$	298	0.380
5	CO_2	$9.48 \cdot 10^4$	0.45	$3.60 \cdot 10^{-7}$	298	0.730
6	CO_2	$9.39 \cdot 10^4$	0.69	$2.89 \cdot 10^{-7}$	298	1.080
7	CO_2	$9.32 \cdot 10^4$	0.16	$3.59 \cdot 10^{-7}$	308	0.210
8	CO_2	$9.32 \cdot 10^4$	0.14	$3.82 \cdot 10^{-7}$	318	0.130
9	CH_4	$9.45 \cdot 10^4$	0.064	$4.50 \cdot 10^{-7}$	298	0.032
10	CH_4	$9.53 \cdot 10^4$	0.14	$4.27 \cdot 10^{-7}$	298	0.069
11	CH_4	$9.45 \cdot 10^4$	0.32	$3.95 \cdot 10^{-7}$	298	0.152
12	CH_4	$9.43 \cdot 10^4$	0.37	$2.57 \cdot 10^{-7}$	298	0.175
13	CH_4	$9.43 \cdot 10^4$	0.39	$4.20 \cdot 10^{-7}$	298	0.163
14	CH_4	$9.41 \cdot 10^4$	0.66	$3.28 \cdot 10^{-7}$	298	0.280
15	CH_4	$9.54 \cdot 10^4$	0.15	$4.45 \cdot 10^{-7}$	308	0.059
16	CH_4	$9.54 \cdot 10^4$	0.14	$4.56 \cdot 10^{-7}$	318	0.050

where W is the weight of adsorbent in the column, Q is the feed volumetric flow rate, C_F is the feed concentration, and t_∞ is a time high enough to consider that the bed is already at equilibrium with the feed concentration. The evolutions of both C and Q at the bed exit are taken into account in the calculation, which were measured experimentally. The adsorbed concentration for each experiment was calculated with Eq. (13). The experimental conditions and the resulting adsorbed concentrations are shown in Table 2.

The adsorption equilibrium data for carbon dioxide and methane on silicalite at 298 K are shown in Figs. 2(a) and (c) respectively.

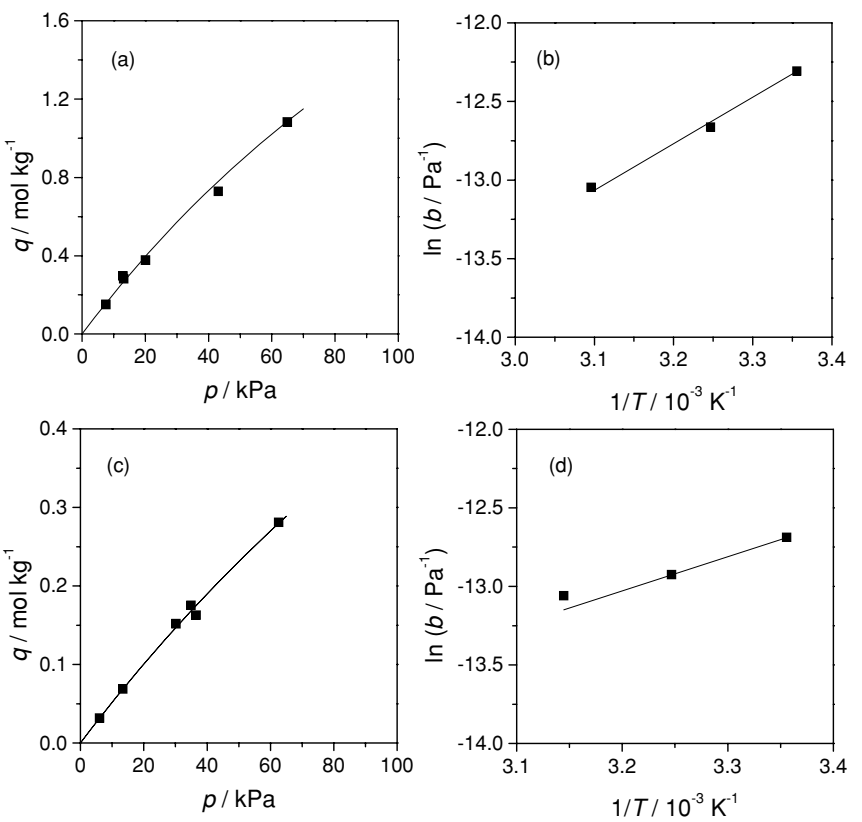

Fig. 2 Adsorption equilibrium data on silicalite. (a) Experimental and fitted equilibrium isotherm for carbon dioxide at 298 K, (b) Arrhenius plot of b for carbon dioxide, (c) Experimental and fitted equilibrium isotherm for methane at 298 K, (d) Arrhenius plot of b for methane

Table 3 Adsorption equilibrium parameters of the Langmuir model on silicalite pellets

Gas	$q_{max}b_{298\,K}$ (mol kg^{-1} Pa^{-1})	q_{max} (mol kg^{-1})	$-\Delta H$ (kJ mol^{-1})
CO_2	$2.16 \cdot 10^{-5}$	4.79	24.6
CH_4	$5.34 \cdot 10^{-6}$	1.73	18.0

These data could be fitted adequately with the Langmuir model ($q = q_{max}bp/(1+bp)$), the model parameters being shown in Table 3.

This model was also fitted to the experimental data obtained at different temperatures in order to estimate the adsorption enthalpy for each adsorbate. The resulting adsorption enthalpies, estimated from the Arrhenius plot of the adsorption affinity versus temperature (Figs. 2(b) and (d)), are given in Table 3, being in good agreement with other reported values (carbon dioxide-silicalite: 24 kJ mol^{-1}, methane-silicalite: 18.6 kJ mol^{-1}, (Golden and Sircar, 1994)). The Henry's constants for carbon dioxide and methane in silicalite pellets are lower than the literature values (for carbon dioxide is about $4 \cdot 10^{-5}$ mol kg^{-1} Pa^{-1} and for methane is about $9 \cdot 10^{-6}$ mol kg^{-1} Pa^{-1} (Golden and Sircar, 1994, Dunne et al., 1996)), which can be attributed to the diluting effect of the binder, combined with some blocking effect.

4.2 Modeling of the breakthrough curves with CO_2-He and CH_4-He mixtures

The breakthrough curves obtained with CO_2-He and CH_4-He mixtures were simulated with the model proposed in the previous section, using the Langmuir equation to describe the adsorption equilibrium isotherm. The values of the physical and transport properties of these gases used for the simulation are shown in Table 4.

The average value of the molecular weight, heat capacity and thermal conductivity of the gas mixture were assumed to be constant, and estimated with the following expression:

$$\overline{pr} = \sum_{i=1}^{i=n} pr_i \cdot \overline{y_i} \tag{14}$$

where pr_i is the corresponding property of the ith component, and $\overline{y_i}$ is the average mole fraction of the component in the bed ($\overline{y_i} = y_{i,feed}/2$, $\overline{y_n} = 1 - \sum_{i=1}^{n-1} \overline{y_i}$). The viscosity of the gas mixture was also assumed constant, and was estimated with the Wilke's equation (Bird et al., 1960). The effect of temperature on viscosity was considered introducing a correction factor (Perry et al., 1999) in the viscosity of the pure components;

$$\mu_i = \mu_{i,ref}\left(\frac{4.58T_0/T_{c,i} - 1.67}{4.58T_{ref}/T_{c,i} - 1.67}\right)^{0.625} \quad T_0/T_{c,i} > 1.5$$
$$\mu_i = \mu_{i,ref}(T_0/T_{ref})^{0.94}T_0/T_{c,i} < 1.5 \tag{15}$$

where T_{ref} is a reference temperature, T_0 is the initial temperature, and T_{ci} is the critical temperature of the ith component. The effect of temperature on the molecular diffusivity was considered in a similar way:

$$D_{i-He} = (D_{i-He})_{ref}(T_0/T_{ref})^{1.75} \tag{16}$$

The value of the LDF parameter of each component was estimated with the expression proposed by Farooq and Ruthven (1990), which considers macropore, micropore and film resistances to mass transfer, adapted to cylindrical pellets,

$$k_{s,i} = \left[\frac{r_p q_{iF}}{2k_f P y_{iF}} + \frac{r_p^2 q_{iF}\tau}{8\varepsilon_{macro}D_{i-He}P\,y_{iF}} + \frac{r_c^2}{15D_c}\right]^{-1} \tag{17}$$

where r_p is the particle radius, k_f is the external mass transfer coefficient, τ is the tortuosity of the macropore

Table 4 Physical properties of carbon dioxide, methane and helium at 293 K (reference temperature)

Gas	M_w (10^{-3} kg mol^{-1})	μ (10^{-5} Pa · s)	c_p (J mol^{-1} K^{-1})[a]	D_{gas-He} (10^{-5} m^2 s^{-1})	k_g (W m^{-1} K^{-1})
CO_2	44	1.50	37.5	5.65	0.0161
CH_4	16	1.07	36.0	6.76	0.0333
He	4	1.84	20.8	–	0.148

[a]The value of c_v was set to $c_p/1.4$

network, r_c is the radius of zeolite crystals, and D_c the intracrystalline diffusivity. The values of this parameter for carbon dioxide, methane and helium in silicalite were taken as 0.2, 0.9 and $3 \cdot 10^{-9}$ m^2 s^{-1}, respectively (Bakker et al., 1997). The external mass transfer coefficient was estimated with the following correlation (Dwivedi and Upadhyay, 1977)

$$k_f = \frac{v_0}{Sc^{2/3}} \left(\frac{0.765}{(Re\varepsilon)^{0.82}} + \frac{0.365}{(Re\varepsilon)^{0.386}} \right) \tag{18}$$

where v_0 is the interstitial velocity, Re is the particle Reynolds number, both calculated with the feed flow rate, and Sc is the Schmidt number. The axial dispersion coefficient was estimated with the correlation of Wakao et al. (1978).

$$D_{L,i} = \frac{D_{m,i}}{\varepsilon}(E_0 + 0.5ScRe) \tag{19}$$

where E_0 is the term corresponding to the stagnant contribution to axial dispersion. As low Reynolds numbers were used in this work (below 0.5), the value of this term has an important effect on the fixed-bed dynamics. This parameter was estimated by fitting the model to the experimental breakthrough curves obtained with carbon dioxide-helium and methane-helium mixtures, resulting in optimum values of 0.23 for carbon dioxide, and 0.30 for methane. Although this parameter is slightly different for carbon dioxide and methane, the quality of fitting achieved using a constant average value of 0.26 for both adsorbates is satisfactory. This value is very close to the one corresponding to an inert bed (0.23), which has previously been observed by other author who has used this correlation for modeling a fixed-bed adsorption process in the gas phase using similar Reynolds numbers (van den Broeke, 1994). It was observed that the variation of adsorbent temperature was noticeable for the experiments with high concentration of carbon dioxide in the feed (an increase of 2 K for run 6). Although this variation is not very high, it must be noted that, as industrial adsorbers are nearly adiabatic (Ruthven et al., 1994), the effect of temperature variation in the adsorber performance can be significant, so this effect was considered in the model. The value of U was set to 30 W m^{-2} K^{-1}, which was used elsewhere for describing the heat transfer between a stainless steel column and the external air in a convective furnace (Da Silva and Rodrigues, 2001). The thermal axial dispersion was estimated with the correlation of Wakao, Kaguei and Nagai (1978), assuming a solid thermal conducitivity/gas thermal conductivity ratio of 10 (Yang, 1997), resulting in $\lambda/k_g = 10 + 0.5RePr$, where Pr is the Prandtl number ($c_p\mu/k_g$). The value of the Nusselt number $h_w d_i/k_g$ was set to 3.66, the value corresponding to laminar flow with constant wall temperature in a circular tube (Sucec, 1975).

The experimental breakthrough curves for carbon dioxide-helium and methane-helium mixtures (conditions in Table 2) were simulated using the model parameter values indicated previously, together with the physical properties given in Table 4. The comparison between experimental and theoretical curves is shown in Fig. 3 for carbon dioxide and in Fig. 4 for methane.

It is observed that the model reproduces the experimental data satisfactorily for the different feed concentrations, flow rates and temperatures used.

4.3 Modeling of the breakthrough curves with CO_2-CH_4 mixtures

The validity of the model for predicting the breakthrough curves obtained with CO_2-CH_4 mixtures was studied. A set of experiments was performed feeding this mixture, the experimental conditions being shown in Table 5.

The experimental curves were predicted describing the multicomponent adsorption equilibrium isotherm with the extended Langmuir equation:

$$\overline{q_i} = \frac{P\, y_i\, \varepsilon_p}{RT\rho_p} + \frac{q_{\max,i}\, f_i\, b_i\, P\, y_i}{1 + \sum_{j=1}^{j=n} f_j\, b_j\, P\, y_j} \tag{20}$$

where the first term accounts for the adsorptive retained in the adsorbent pores, and f_i are empirical interac-

Table 5 Experimental conditions for the runs performed with carbon dioxide-methane mixtures

Run	P_0 (Pa)	y_{FCO_2}	Q (m^3 s^{-1})	T (K)
17	$9.51 \cdot 10^4$	0.157	$2.85 \cdot 10^{-7}$	298
18	$9.55 \cdot 10^4$	0.270	$2.77 \cdot 10^{-7}$	298
19	$9.53 \cdot 10^4$	0.390	$2.74 \cdot 10^{-7}$	298
20	$9.47 \cdot 10^4$	0.550	$2.97 \cdot 10^{-7}$	299
21	$9.55 \cdot 10^4$	0.270	$2.82 \cdot 10^{-7}$	308
22	$9.45 \cdot 10^4$	0.270	$2.79 \cdot 10^{-7}$	318

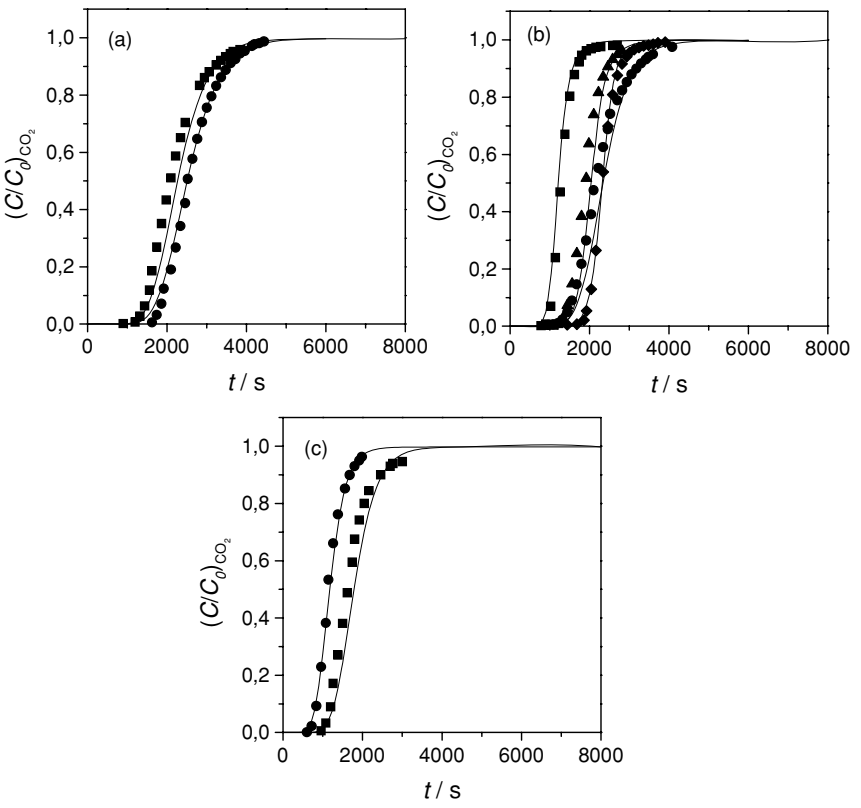

Fig. 3 Breakthrough curves of CO_2-He mixtures in silicalite. Experimental conditions in Table 2. Continuous lines are obtained with the model. (a) squares, Run 1; circles, Run 2. (b) squares, Run 3; circles, Run 4; triangles, Run 5; diamonds, Run 6. (c) squares, Run 7; circles, Run 8

tion factors taking into account the possible lateral interactions between the adsorbates in the adsorbed phase. The CO_2-CH_4 diffusivity was estimated as $1.6 \cdot 10^{-5}$ m^2 s^{-1} at 293 K. In a first test, the experimental breakthrough curves were reproduced setting the interaction factors to 1. The comparison between experimental and theoretical curves is shown in Fig. 5 (dashed lines).

It is observed that the model describes adequately the breakthrough curves for the experiments with low carbon dioxide concentration, whereas the error is higher for the runs with higher carbon dioxide concentration (runs 19 and 20). In order to improve the quality of the prediction, the model was fitted to all the experimental curves leaving the interaction factors as adjustable parameters, resulting in $f_{CO_2} = 0.90$ and $f_{CH_4} = 0.49$. The breakthrough curves calculated with these interaction factors (continuous lines in Fig. 5) give a better description of the full set of experimental data. These values of the interaction factors lead to higher carbon dioxide/methane selectivity than the one calculated with the extended Langmuir equation in its predictive form, which has already been observed elsewhere for ZSM-5 zeolite with low aluminum content (Harlick and Tezel, 2003). This result is attributed to the lateral interactions between carbon dioxide molecules, which are much stronger than the ones between methane molecules, due to its high quadrupole moment. A sensitivity study was performed in order to determine the importance of the mass transfer resistance in the bed performance. Fig. 6 shows a comparison between the experimental breakthrough curve obtained in run 17 (Table 5) and the predicted curves obtained with the mass transfer coefficient of carbon dioxide and methane multiplied by 0.1, 1 and 10.

It is observed that the breakthrough curve changes very little when the LDF parameter is increased, but the change is noticeable when it is decreased. Therefore, although it cannot be ensured that the LDF parameter estimated with Equation (17) accounts for the mass transfer resistance accurately, it can be stated that the real value of this parameter is equal or higher than the estimated one. It is also deduced that the mass transfer resistance is not a controlling step in

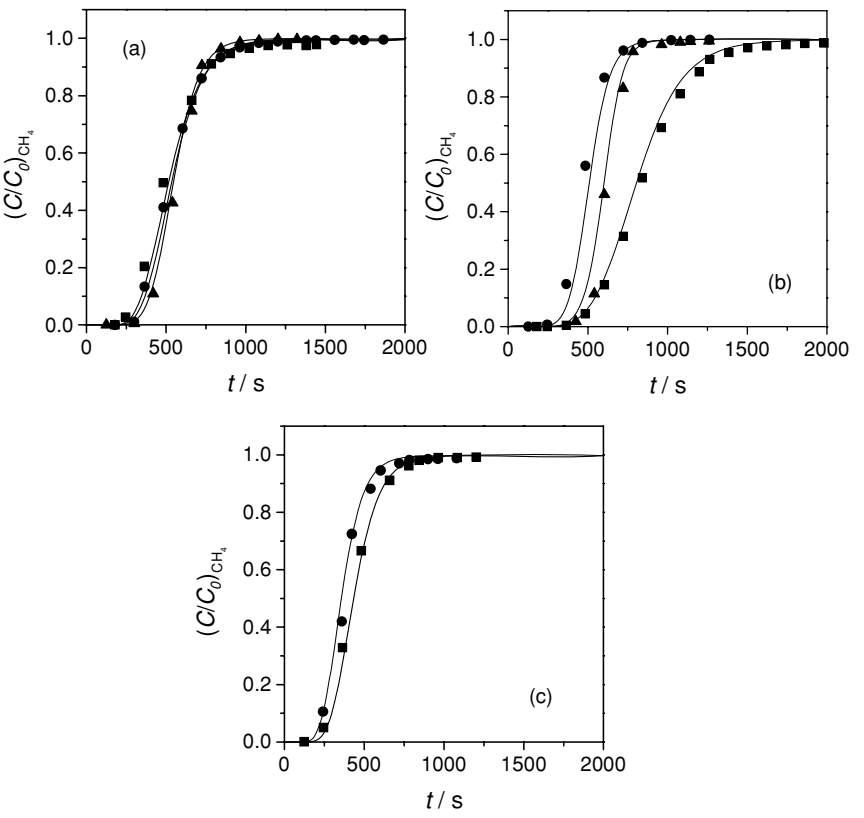

Fig. 4 Breakthrough curves of CH_4-He mixtures in silicalite. Experimental conditions in Table 2. Continuous lines are obtained with the model. (a) squares, Run 9; circles, Run 10; triangles, Run 11. (b) squares, Run 12; circles, Run 13; triangles, Run 14. (c) squares, Run 15; circles, Run 16

these system, and that the spread of the mass transfer zone is due to the axial dispersion only, for the contact times used in the experiments. However, the mass transfer resistance could be relevant for shorter contact times.

4.4 Simulation of the carbon dioxide/methane separation by PSA

A PSA cycle was proposed to increase the methane content of a carbon dioxide/methane mixture using silicalite as the sorbent, which consisted of two twin beds passing through four consecutive steps: (i) pressurization with feed, (ii) feed at high pressure, (iii) countercurrent blowdown and (iv) countercurrent purge with part of the product at low pressure. The pressurization and blowdown steps have the same duration, and the same applies to the feed and purge steps. A scheme of the cycle is shown in Fig. 7.

As methane is the weak adsorbate, it is obtained as the purified product in the feed step.

For the pressurization the boundary conditions were the following:

$$\begin{aligned} &\text{Open end } P|_{z^+} = P_H + (P_L - P_H)\exp(-k_{pres}t) \\ &\text{Closed end } \left.\frac{\partial P}{\partial x}\right|_{z-} = 0 \end{aligned} \tag{21}$$

$$\begin{aligned} &\text{Open end } -\varepsilon\frac{D_L}{L}C\left.\frac{\partial y_i}{\partial x}\right|_{z^+} + u\,C(y_i|_{z^+} - y_i|_{z^-}) = 0 \\ &\text{Closed end } \left.\frac{\partial y_i}{\partial x}\right|_{z^-} = 0 \end{aligned} \tag{22}$$

$$\begin{aligned} &\text{Open end } -\frac{\lambda}{L}\left.\frac{\partial T_g}{\partial x}\right|_{z^+} + u\,C c_{p,g}(T_g|_{z^+} - T_g|_{z^-}) = 0 \\ &\text{Closed end } \left.\frac{\partial T_g}{\partial x}\right|_{z^-} = 0 \end{aligned} \tag{23}$$

where k_{pres} is a parameter describing the rate of pressurization. For the blowdown step, the boundary

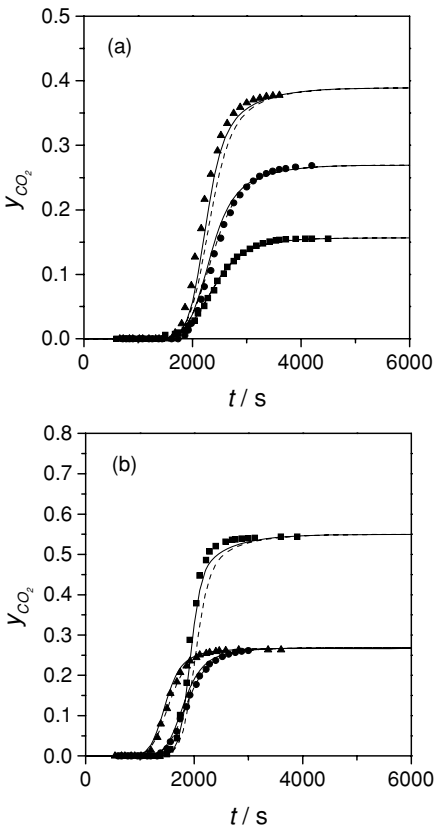

Fig. 5 Breakthrough curves of CO_2-CH_4 mixtures in silicalite. Experimental conditions in Table 5. Continuous and dashed lines are obtained with and without interaction factors, respectively (Eq. (20)). (a) squares, Run 17; circles, Run 18; triangles, Run 19. (b) squares, Run 20; circles, Run 21; triangles, Run 22

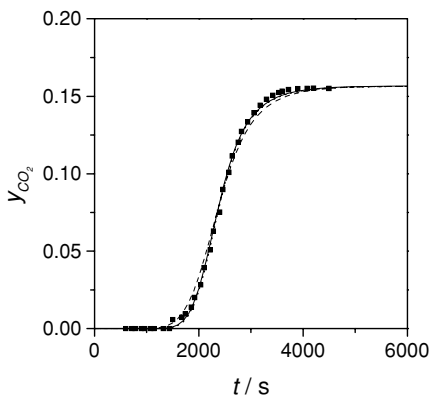

Fig. 6 Comparison between the experimental breakthrough curve obtained in Run 17 (squares) and the predicted curves obtained with the mass transfer coefficient of carbon dioxide and methane multiplied by 0.1 (dashed line), 1 (continuous line) and 10 (dotted line)

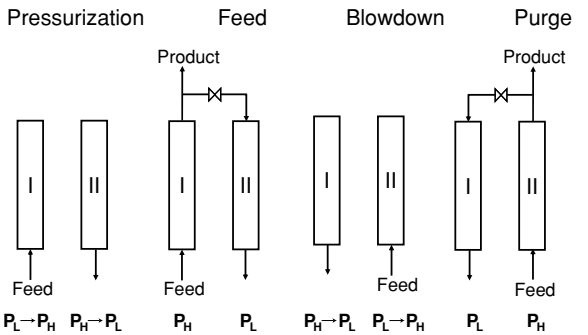

Fig. 7 Scheme of the PSA cycle proposed in this work. The name of the step is referred to bed I. P_L and P_H are low and high pressures

conditions were:

$$\text{Open end } P|_{z^-} = P_L + (P_H - P_L)\exp(-k_{pres}t)$$
$$\text{Closed end } \left.\frac{\partial P}{\partial x}\right|_{z^+} = 0 \tag{24}$$

$$\text{Open end } \left.\frac{\partial y_i}{\partial x}\right|_{z^-} = 0$$
$$\text{Closed end } \left.\frac{\partial y_i}{\partial x}\right|_{z^+} = 0 \tag{25}$$

$$\text{Open end } \left.\frac{\partial T_g}{\partial x}\right|_{z^-} = 0$$
$$\text{Closed end } \left.\frac{\partial T_g}{\partial x}\right|_{z^+} = 0 \tag{26}$$

For the feed step, the boundary conditions are given by Eqs. (9–11). For the purge step, the conditions are the same except for the entrance and exit positions. The initial condition for both beds is that they are equilibrated with the feed mixture at P_L. The performance of the PSA cycle was evaluated by estimating the product purity, recovery and productivity when the cycle has reached the steady state, which were calculated with the following expressions:

$$\text{Product purity} = \frac{\text{mol of } CH_4 \text{ in product}}{(\text{mol of } CO_2 + \text{mol of } CH_4) \text{ in product}} \tag{27}$$

$$\text{Recovery} = \frac{\text{mol of } CH_4 \text{ in product}}{\text{mol of } CH_4 \text{ in feed}} \tag{28}$$

$$\text{Productivity} = \frac{\text{kg of } CH_4 \text{ in product}}{(t_{pres} + t_{feed} + t_{blow} + t_{purge})\, 2W} \tag{29}$$

Table 6 Bed dimensions and operating conditions for PSA simulations

Bed length	$L = 0.2\,\text{m}$
High pressure	$P_H = 1 \cdot 10^5\,\text{Pa}$
Low pressure	$P_L = 1 \cdot 10^4\,\text{Pa}$
Bed internal diameter	$d_i = 0.04\,\text{m}$
Pressurization rate constant	$k_{pres} = 0.4\,\text{s}^{-1}$
Pressurization time	$t_{pres} = 20\,\text{s}$
Blowdown time	$t_{blow} = 20\,\text{s}$
Feed superficial velocity	$u_F = 0.05\,\text{m s}^{-1}$
Feed temperature	298 K

where t_{pres}, t_{feed}, t_{blow}, and t_{purge} are the pressurization, feed, blowdown and purge times, respectively.

The simulations were performed for different values of the feed composition (38 and 50% methane), feed times and feed to purge velocity ratios. The bed dimensions and operating conditions which were kept constant for the PSA simulations are given in Table 6.

The rest of parameters not given in these tables are the same as the ones used in the reproduction of the breakthrough curves of carbon dioxide-methane mixtures. The resulting values of the performance parameters at the steady state are given in Table 7.

The steady state was reached after 5 cycles. Simulation 2 was performed setting the heat transfer coefficients to a very high value, so the beds are isothermal in this case. It is observed that product purity increases with the purge to feed velocity ratio. This ratio is equivalent to the one between the gas volumes used in each step in this cycle. This increase is due to the fact that the carbon dioxide adsorption front formed in the feed step moves a larger distance backwards in the purge step when the purge gas volume (with high methane concentration) is increased. Similarly, the product purity decreases with the feed time, because the carbon dioxide adsorption front advances more in the feed step. The recovery decreases when the product purity is increased because more methane must be left in the bed in the blowdown and purge steps to obtain a better purity. By comparing simulations 1, 3 and 5, it is deduced that, to increase the product purity, it is better to increase the purge to feed velocity ratio rather than decreasing the feed time, because higher purity, recovery and productivity are obtained in the first case. By comparing simulations 1 and 2, it is observed that the heat effects are significant and detrimental to the separation, so they must be taken into account. With the conditions of simulation 1, 98% methane purity can be reached from a 38% carbon dioxide feed, with 54% recovery, and with a productivity of $0.16\,\text{kg}_{\text{methane}}\,\text{kg}^{-1}_{\text{sorbent}}\,\text{h}^{-1}$. The cycle can also treat a feed with 50% carbon dioxide concentration (simulation 7), with a little lower recovery and productivity (52% and $0.13\,\text{kg}_{\text{methane}}\,\text{kg}^{-1}_{\text{sorbent}}\,\text{h}^{-1}$). These results are comparable to ones reported in the literature with other systems, both simulated and experimental, taking into account that these parameters depend on the pressure ratio used in the PSA system ($P_H/P_L = 10$ in this work): (i) purity = 90%, recovery = 90%, $P_H/P_L = 8.49$, experimental data by Kapoor and Yang (1989) using Bergbau Forschung carbon molecular sieve, (ii) purity = 95.5%, recovery = 40%, $P_H/P_L = 10.94$, simulated data in the same work, (iii) purity = 97.1%, recovery = 79.4%, $P_H/P_L = 32$, experimental data by Cavenati et al. (2005) using Takeda Carbon Molecular Sieve 3A, (iv) purity = 97.9%, recovery = 68.1%, $P_H/P_L = 40$, simulated data in the same work. From this comparison, it can be stated that silicalite can also be a suitable adsorbent for employment in a PSA separation process for carbon dioxide removal from coalseam and landfill gases. It must be noted that the present results have been obtained using a model which has been validated

Table 7 Performance of the proposed PSA cycle for different operating conditions

Simulation	CO_2 mol fraction in feed (%)	[a]u_P/u_F	t_{feed} (s)	Product purity (%)	Recovery (%)	Productivity ($\text{kg}_{\text{methane}}\,\text{kg}^{-1}_{\text{sorbent}}\,\text{h}^{-1}$)
1	0.38	1.55	25	98.0	54.1	0.165
[b]2	0.38	1.55	25	98.9	47.9	0.154
3	0.38	2.00	25	98.7	50.2	0.153
4	0.38	1.00	25	96.0	58.9	0.179
5	0.38	1.55	20	98.1	48.4	0.144
6	0.38	1.55	30	97.8	58.5	0.181
7	0.50	1.80	25	98.1	52.0	0.135

[a]Purge to feed velocity ratio.
[b]Simulated in isothermal conditions.

performing breakthrough experiments with breakthrough times (1000–1800 s) higher than the ones corresponding to the PSA simulations (20–30 s). The effect of mass transfer resistance is more noticeable the shorter is the breakthrough time. Thus, although it was observed that the mass transfer resistance was not relevant in the breakthrough experiments used in the model validation, it may be argued that this is not valid for the conditions used in the PSA simulations, so the PSA system may be kinetics-controlled. However, the sensitivity analysis performed in the previous section showed that the actual mass transfer resistance in this system is lower or equal than the one considered in the model. Therefore, although the model may not predict correctly PSA performance, the real results must be better or equal than the ones obtained with the model, but not worse.

5 Conclusions

The adsorption of carbon dioxide and methane on silicalite pellets packed in a fixed bed has been studied. Equilibrium and kinetic measurements of the adsorption of carbon dioxide and methane have been carried out, and the monocomponent adsorption equilibrium isotherms have been obtained for both gases. A model based on the LDF approximation for the mass transfer was able to describe the breakthrough curves obtained experimentally. For carbon dioxide/methane mixtures, the multicomponent adsorption isotherm was reproduced with the extended Langmuir model with empirical interaction factors. From this isotherm equation, it is deduced that the carbon dioxide/methane selectivity of silicalite is higher than the one predicted with the extended Langmuir model based on the pure adsorption isotherms.

A PSA cycle was proposed for obtaining methane with a purity higher than 98% from carbon dioxide/methane mixtures containing 38% and 50% methane, and its performance was simulated. The simulation results show that silicalite can be a suitable adsorbent for carbon dioxide removal from coalseam and landfill gases in a PSA separation process.

Acknowledgement Financial support from the "Ministerio de Educación y Ciencia" of Spain through project CTQ2004-00320/PPQ is gratefully acknowledged.

Notation

b = adsorption affinity, Pa^{-1}
C = total gas concentration, mol m^{-3}
C_F = feed concentration of the adsorbate, mol m^{-3}
c_p = heat capacity at constant pressure, J mol^{-1} K^{-1}
c_v = heat capacity at constant volume, J mol^{-1} K^{-1}
D = diffusivity, m^2 s^{-1}
D_L = axial dispersion coefficient, m^2 s^{-1}
d_p = particle diameter, m
E_0 = stagnant contribution to axial dispersion
f = empirical interaction parameter
h_w = heat transfer coefficient between the gas and the wall, W m^{-2} K^{-1}
ΔH = adsorption enthalpy, J mol^{-1}
k_f = external mass transfer coefficient, m s^{-1}
k_g = gas conductivity, W m^{-1} K^{-1}
k_{pres} = pressurization rate parameter, s^{-1}
k_s = lumped mass transfer coefficient, s^{-1}
L = bed length, m
N = adsorption rate, mol m^{-3} s^{-1}
P = pressure, Pa
Pr = Prandtl number, $c_p\mu/k_g$
Q = volumetric flow rate, m^3 s^{-1}
q^* = adsorbed concentration in equilibrium with the gas phase, mol kg^{-1}
$\overline{q}$ = average adsorbed concentration, mol kg^{-1}
q_{max} = maximum adsorption capacity, mol kg^{-1}
R = gas constant, 8.31 J mol^{-1} K^{-1}
r_c = radius of zeolite crystals, m
Re = particle Reynolds number, $v_0\rho_g d_p/\mu$
R_i = bed radius, m
R_{ml} = log mean wall radius, m
r_p = particle radius, m
Sc = Schmidt number, $\mu/(\rho_g D_m)$
t = time, s
T = temperature, K
U = overall heat transfer coefficient between the wall and the external air, W m^{-2} K^{-1}
u = superficial velocity, m s^{-1}
v_0 = interstitial velocity, m s^{-1}
W = weigh of sorbent, kg
x = dimensionless axial coordinate
y = mole fraction in the gas phase

Greek symbols

ε = bed voidage fraction
λ = thermal axial dispersion coefficient, W m^{-1} K^{-1}
μ = gas viscosity, Pa s
ρ = density, kg m^{-3}
τ = tortuosity

Subscripts and superscripts

0 = initial
c = intracrystalline
ext = external air
F = feed conditions
g = gas
H = high pressure
i = ith component
L = low pressure
m = molecular
macro = macropores
micro = micropores
ml = log mean
s = solid
w = wall

References

Bakker, W.J.W., L.J.P. van den Broeke, F. Kapteijn, and J.A. Moulijn, "Temperature Dependence of One-component Permeation through a Silicalite-1 Membrane," *AIChE J.*, **43**, 2203–2213 (1997).

Bird, R.B., W.E. Stewart, and E.N. Lightfoot, *Transport Phenomena*, Wiley, New York, 1960.

Cavenati, S., C.A. Grande, and A.E. Rodrigues, "Adsorption Equilibrium of Methane, Carbon Dioxide, and Nitrogen on Zeolite 13X at High Pressures," *J. Chem. Eng. Data*, **49**, 1095–1101 (2004).

Cavenati, S., C.A. Grande, and A.E. Rodrigues, "Upgrade of Methane from Landfill Gas by Pressure Swing Adsorption," *Energy & Fuels*, **19**, 2545–2555 (2005).

Da Silva, F. and A.E. Rodrigues, "Propylene/Propane Separation by Vacuum Swing Adsorption Using 13X Zeolite," *AIChE J.*, **47**, 341–357 (2001).

Delgado, J.A., T.A. Nijhuis, F. Kapteijn, and J.A. Moulijn, "Modeling of Fast Pulse Responses in the Multitrack: and Advanced TAP Reactor," *Chem. Engng. Sci.*, **57**, 1835–1847 (2002).

Dunne, J.A., R. Mariwala, M. Rao, S. Sircar, R.J. Gorte, and A.L. Myers, "Calorimetric Heats of Adsorption and Adsorption Isotherms. 1. O_2, N_2, Ar, CO_2, CH_4, C_2H_6, and SF_6 on Silicalite," *Langmuir*, **12**, 5888–5895 (1996).

Dwivedi, P.N. and S.N. Upadhyay, "Particle-Fluid Mass Transfer in Fixed and Fluidized Beds," *Ind. Eng. Chem. Process Des. Dev.*, **16**, 157–165 (1977).

Engelhard Corporation, *Adsorption Processes for Natural Gas Treatment, A Technology Update*, www.engelhard.com, 2005.

Farooq, S. and D.M. Ruthven, "Heat Effects in Adsorption Column Dynamics. 1. Comparison of One- and Two-Dimensional Models," *Ind. Eng. Chem. Res.*, **29**, 1076–1084 (1990).

Golden, T.C. and S. Sircar, "Gas Adsorption on Silicalite," *J. Colloid Interface Sci.*, **162**, 182–188 (1994).

Gomes, V.G. and M.M. Hassan, "Coalseam methane recovery by vacuum swing adsorption," *Sep. Purif. Technol.*, **24**, 189–196 (2001).

Harlick, P.J.E. and F.H. Tezel, "Adsorption of Carbon Dioxide, Methane and Nitrogen: Pure and Binary Mixture Adsorption for ZSM-5 with SiO_2/Al_2O_3 ratio of 280," *Sep. Purif. Technol.*, **33**, 199–210 (2003).

Kapoor, A. and R.T. Yang, "Kinetic Separation of Methane-Carbon Dioxide Mixture By Adsorption on Molecular Sieve Carbon," *Chem. Engng. Sci.*, **44**, 1723–1733 (1989).

Li, S., J.G. Martinek, and J.L. Falconer, "High-Pressure CO_2/CH_4 Separation Using SAPO-34 Membranes," *Ind. Chem. Eng. Res.*, **44**, 3220–3228 (2005).

Madsen, N.K. and R.F. Sincovec, "PDECOL, General Collocation Software for Partial Differential Equations [D3]," *ACM Trans. Math. Software*, **5**, 326–351 (1979).

Perry, R.H., D.W. Green, and J.O. Maloney, (Eds.), *Perry's Chemical Engineers' Handbook (7th edition)*, McGraw-Hill, New York, 1999.

Pilarczyk, E. and K. Knoblauch, *Separation Technology*, N. Li and H. Strathmann, (Eds.), p. 522, Eng. Foundation, New York, 1988.

Ruthven, D.M., S. Farooq, and K.S. Knaebel, *Pressure Swing Adsorption*, Chapter 2 and pp. 208, 244, VCH, New York, 1994.

Schroter, H.J. and H. Juntgen, *Adsorption: Science and Technology*, p. 269, NATO ASI 158, A.E. Rodrigues, M.D. LeVan, and D. Tondeur (Eds.), Kluwer, Dordrecht, 1989.

Sircar, S. and J.W. Zondlo, Hydrogen Purification by Selective Adsorption, US Patent 4,077,779, 1978.

Sucec, J., *Heat Transfer*, p. 371, Simon and Schuster Inc., New York, 1975.

Suzuki, T., A. Sakoda, M. Suzuki, and J. Izumi, "Adsorption of Carbon Dioxide onto Hydrophobic Zeolite Under High Moisture," *J. Chem. Eng. Japan*, **30**, 954–958 (1997).

van den Broeke, L.J.P., *The Maxwell-Stefan theory for micropore diffusion*, Ph D. Thesis, p. 132, University of Amsterdam, 1994.

Wakao, N., S. Kaguei, and H. Nagai, "Effective Diffusion Coefficients for Fluid Species Reacting with First Order Kinetics in Packed Bed Reactors and Discussion on Evaluation of Catalyst Effectiveness Factors," *Chem. Engng. Sci.*, **33**, 183–187 (1978).

Yang, R.T., *Gas Separation by Adsorption Processes*, pp. 4 and 124, Imperial College Press, Singapore, 1997.